

Room temperature spontaneous emission enhancement from quantum dots in photonic crystal slab cavities in the telecommunications C-band

R. Hostein, R. Braive, M. Larqué, K.-H. Lee, A. Talneau,

L. Le Gratiet, I. Robert-Philip, I. Sagnes, and A. Beveratos

Laboratoire de Photonique et Nanostructures LPN-CNRS UPR-20

Route de Nozay. 91460 Marcoussis, France

(Dated: March 25, 2009)

Abstract

We report on the control of the spontaneous emission dynamics from InAsP self-assembled quantum dots emitting in the telecommunications C-band and weakly coupled to the mode of a double heterostructure cavity etched on a suspended InP membrane at room temperature. The quality factor of the cavity mode is 44×10^3 with an ultra-low modal volume of the order of $1.2 (\lambda/n)^3$, inducing an enhancement of the spontaneous emission rate of up a factor of 2.8 at 300 K.

The spontaneous emission dynamics of a single emitting dipole results from the interaction between the emitting dipole and its electromagnetic environment. Consequently, the modification of the electromagnetic field around the point emitter, by use of a microcavity for instance, alters the spontaneous emission lifetime of the emitting dipole, inducing in the weak coupling regime either an enhancement or an inhibition of the spontaneous emission rates [1]. First observed in atom physics [2, 3], the transposition of these effects to semiconductor physics has already been demonstrated by embedding, for instance, self-assembled quantum dots in micropillars [4, 5, 6], microdisks [7, 8, 9] and more recently photonic crystal slab cavities [10, 11, 12]. Such spontaneous emission modification can be used to increase the modulation bandwidth of nanolasers [13] or the quantum efficiency of single photon sources for quantum communication [14]. However, most of these experimental demonstrations involve InAs/GaAs quantum dots emitting below 1050 nm and at low temperature, while such prospective applications require operation in the telecommunication wavelength range and at room temperature. Recently, spontaneous emission enhancement by a factor of 8 has been observed at low temperature on InAs/GaAs dots emitting in the telecommunication O-band (1260 – 1360 nm) [15]. The remaining concern is room temperature operation. At room temperature, spontaneous emission enhancement is limited by the large homogeneous linewidth of emitting dipoles but may be increased in a simple manner by reducing the modal volume of the cavity mode, which is a particular feature of photonic crystals. Up to now, most experiment aiming at observing a Purcell effect at room temperature by use of photonic crystals were based on an analysis of the amplitude of the emitted signal, in order to infer an estimated value of the Purcell factor [16, 17]. Yet, direct lifetime measurements solely allow to unambiguously determine the amplitude of the spontaneous emission exaltation induced by the presence of the microcavity. In this paper, we report on lifetime measurements indicating a spontaneous emission enhancement by a factor of 2.8 at room temperature on an ensemble of quantum dots emitting at 1538 nm.

Samples are grown by metalorganic vapour phase epitaxy. The InP membrane is grown on a GaInAs sacrificial layer lying on a InP buffer. It incorporates in its center a single layer of self-assembled InAsP quantum dots. The quantum dots density is of the order of $15 \times 10^9 \text{ cm}^{-2}$ and their photoluminescence is centered around 1560 nm at 300 K, with a inhomogeneous spectral broadening of the order of 150 nm [18]. After the deposit of a SiN layer on top of the semiconductor, the cavity pattern is defined on a layer of polymethylmethacrylate (PMMA) using direct-write electron-beam lithography. The cavity is formed by a double heterostructure resonator [19]. It consists of a W1 waveguide composed of one missing row of holes in the ΓK direction of a hexagonal lattice structure, with a local enhancement of the lattice period over two periods at the center of the photonic crystal waveguide. The lattice period is only modified along the ΓK direction. The waveguide with the

larger longitudinal lattice constant $a_c = 440$ nm forms the nanocavity closed by two surrounding mirror waveguides with smaller lattice constant $a_m = 410$ nm. The target air hole-radius r/a_m is 0.293. The semiconductor is etched using Inductive Coupled Plasma [20, 21], followed by wet etching and supercritical drying in order to leave the membrane suspended in air.

The samples are studied at room temperature. Optical excitation is provided by either a continuous wave (CW) 532 nm Nd:YAG laser or a pulsed Ti:Sa laser emitting at 840 nm with a repetition rate of 80 MHz and a 5 ps pulse width. The pumping laser is focused to a $5\text{ }\mu\text{m}$ spot on the sample by a microscope objective (Numerical Aperture = 0.4). The luminescence is collected by the same microscope objective and separated from the pumping laser by means of a dichroic mirror and an antireflection coated silicon filter. The spontaneous emission is spectrally dispersed by a 0.5 m spectrometer with a spectral resolution of 0.15 nm and detected by a cooled InGaAs photodiodes array (Roper Scientific). Emission linewidths smaller than 0.15 nm are measured by interferometric analysis of the emitted light on a Michelson interferometer added in the photoluminescence path. The linewidth is inferred after fitting the interference fringes envelope by the Fourier transform of a Lorentzian function (see Fig. 1). Lifetime measurements under pulsed excitation are obtained by means of a superconducting single photon counter (SSPD-Scontel) with a time resolution of $\sqrt{2}\sigma = 70$ ps, a quantum efficiency of 3% at $1.55\text{ }\mu\text{m}$ and dark count rates lower than 30 counts.s^{-1} . The histograms of the time intervals between the detection of a photon emitted by the sample after one excitation pulse and the next laser excitation pulse are recorded on a Lecroy 8620A oscilloscope. Before being detected by the superconducting detector, the emission light is filtered by a tunable filter (Santec, 0.4 nm bandwidth, 20 dB extinction rate).

In order to deduce the bare quality factor Q_{cav} of the cavity mode, we performed linewidth measurements as a function of the pump power under continuous excitation. Figure 2 represents the evolution of the linewidth (left scale) and the integrated output intensity (right scale) as function of the pump power. The linewidth exponentially decreases up to a pump power of $385\text{ }\mu\text{W}$. Above this excitation power, the linewidth decrease is slower and the output power increases non-linearly, probably indicating the onset of lasing. From linewidth measurements at an excitation power of $385\text{ }\mu\text{W}$ corresponding to the transparency of the gain medium, we extract a cavity quality factor Q_{cav} of 44000.

In order to quantify the acceleration of the quantum dots spontaneous emission rate induced by the cavity, we perform time-resolved measurements under pulsed excitation. The sample is excited with $18\text{ }\mu\text{W}$ average power. Such pulsed excitation power corresponds to the quantum dots transparency. The measured lifetimes of the quantum dots respectively off resonance (in the unprocessed sample) and on resonance with the cavity mode are shown on Fig. 3. Both decay curves display a double

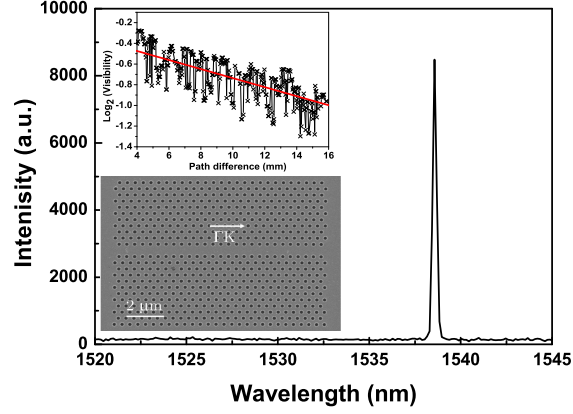


FIG. 1: Typical microphotoluminescence spectrum obtained under CW excitation from the double heterostructure cavity exhibiting a resonant peak at a wavelength of 1538 nm. Inset (above): Interferogram contrast of the emitted light decaying exponentially (gray stars and black solid line: experimental data and red solid line: exponential fit). The excitation power after the microscope objective is 385 μW . Inset (below) : top view of the photonic crystal cavity.

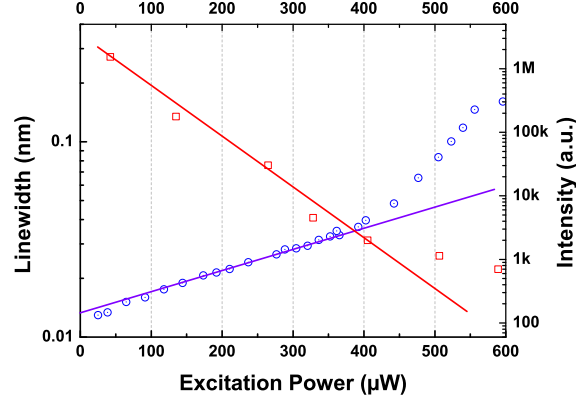


FIG. 2: (Left axis) Red squares: Linewidth of the cavity mode as function of the excitation power. (Right axis) Blue circles: Emission output intensity as function of the excitation power. Solid lines are guides for the eye. Onset of lasing can be observed, for excitation powers above 385 μW .

exponential decay. We attribute the fast decay to the emission of excited states (such as an electron-hole pair on the p shell) of lower energy quantum dots and the long decay time to the emission of quantum dots ground state [22]. The double exponential feature disappears at low power and low temperature but is always observed at room temperature for any excitation power due to thermal population of the p-shell. These decay times τ_j^i ($j = 0$ or *cav* for dots respectively off and on resonance with the cavity mode; $i = f, l$ for fast and long decay respectively) can be inferred from

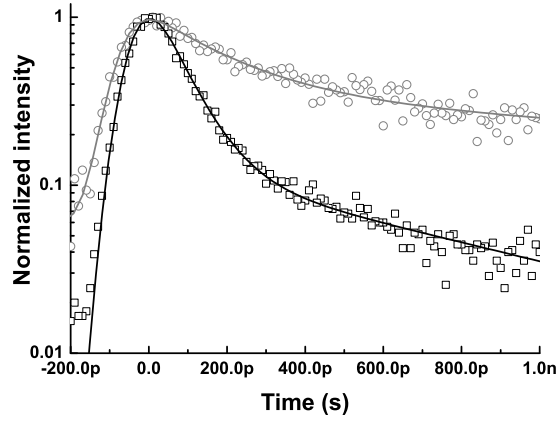


FIG. 3: Lifetime measurements on ensemble of quantum dots over a spectral window of 0.8 nm centered at $\lambda = 1538$ nm. Empty (resp. full) circles represent the lifetime measured on dots off (resp. on) resonance with the cavity mode. Dotted line and solid line are fits obtained by use of equation 1 for dots respectively off and on resonance.

	Unprocessed sample ($j = 0$)	Cavity mode ($j = cav$)	τ_{cav}^i/τ_0^i
Long decay ($i = l$)	2.14 ± 0.28 ns	0.77 ± 0.06 ns	2.8 ± 0.6
Fast decay ($i = f$)	0.20 ± 0.02 ns	0.07 ± 0.03 ns	2.6 ± 0.3

TABLE I: Measured spontaneous emission decay times for the dots in the unprocessed sample and on resonance with the cavity mode.

fits by bi-exponential decay curves taking in account the timing resolution of the detector as follows:

$$I(t) = \sum_{i=s,l} a_i e^{\frac{\sigma^2}{2(\tau_j^i)^2} - \frac{t}{\tau_j^i}} \left(1 - \text{Erf} \left(\frac{\sigma^2 - t\tau_j^i}{\sqrt{2}\sigma\tau_j^i} \right) \right) \quad (1)$$

The inferred values of the different decay times are summarized in table I. The ratio τ_{cav}^i/τ_0^i between the observed spontaneous emission decay times in the cavity mode and in unprocessed sample for both long and short decays allows us to determine the minimal spontaneous emission enhancement F induced by the cavity, which is of the order of 2.8. In our experiment, the cavity linewidth is smaller than the homogeneous linewidth $\delta\lambda_{em}$ of the quantum dot optical transition at room temperature. The Purcell factor is hence limited by the quantum dot linewidth and not the cavity linewidth [23, 24]. We can define an equivalent quantum dot quality factor Q_{em} as the ratio $\lambda/\delta\lambda_{em}$. In this context, the measured spontaneous emission enhancement factor on ensemble of quantum dots is equal to:

$$F = \frac{1}{2} \frac{\int_S |\vec{E}(x, y)|^4 dx dy}{|\vec{E}(x, y)|_{max}^2 \int_S |\vec{E}(x, y)|^2 dx dy} F_p \quad (2)$$

$$\text{with } F_p = \frac{3}{4\pi^2} \frac{Q_{em}(\lambda/n)^3}{V_{eff}} \quad (3)$$

The first term $1/2$ in the expression of F results from the random orientation of the optical emitting dipoles in the quantum dot plane S and the second term accounts for the random spatial distribution of the dots in the central plane of the membrane, estimated to 0.17 from our FDTD simulations. The last term F_p is the maximal Purcell factor achieved for a single spatially and spectrally resonant quantum dot with an optical dipole collinear to the electric field \vec{E} in the cavity central plane. The effective volume of the cavity mode has been estimated by FDTD simulations to $V_{eff} = 1.2(\lambda/n)^3$. Consequently, $F = Q_{em}/186$, which corresponds to a Q_{em} of the order of 500 regarding our measured F values of 2.7. This value of Q_{em} corresponds to a $\delta\lambda_{em}$ of the order of 3 nm at 300 K, which is rather small compared to InAs/GaAs quantum dots, but may arise from the large dimensions of the dots [25] (of the order of 8 monolayers height and 40 nm large [18]). Moreover, this value of Q_{em} indicates that the spontaneous emission enhancement for such dots at room temperature would be at most equal to $1/2 \times F_p \simeq 30$.

In conclusion, we demonstrated spontaneous emission enhancement from ensemble of InAsP quantum dots emitting in the telecommunication C-band at room temperature. This spontaneous emission exaltation results mainly from the coupling of dots in a small mode volume double heterostructure cavity, which displays a single mode with a quality factor of 44000. The enhancement by a factor of the order of three of the spontaneous emission dynamics is limited by the homogeneous linewidth of the quantum dots at room temperature. The authors acknowledge financial support from Conseil régional d’Île-de-France under CRYPHO project.

-
- [1] E. Purcell, Phys. Rev. **69** 681 (1946)
 - [2] P. Goy, J. M. Raymond, M. Gross and S. Haroche, Phys. Rev. Lett. **50** 1903 (1983)
 - [3] R. G. Hulet, E. S. Hilfer and D. Kleppner, Phys. Rev. Lett. **55** 2137 (1985)
 - [4] J. M. Gérard, B. Sermage, B. Gayral, B. Legrand, E. Costard and V. Thierry-Mieg, Phys. Rev. Lett. **81** 1110 (1998)
 - [5] M. Bayer, T. L. Reinecke, F. Weidner, A. Larionov, A. McDonald and A. Forchel, Phys. Rev. Lett. **86**, 3168 (2001)
 - [6] G. S. Solomon, M. Pelton, Y. Yamamoto, Phys. Rev. Lett. **86**, 3903 (2001)
 - [7] J.-M. Gérard and B. Gayral, J. Lightwave Technol. **17**, 2089 (1999)
 - [8] A. Kiraz, P. Michler, C. Becher, B. Gayral, A. Imamoglu, L. Zhang, E. Hu, W. V. Schoenfeld and P. M. Petroff, Appl. Phys. Lett. **78**, 3932 (2001)

- [9] W. Fang, J. Y. Xu, A. Yamilov, H. Cao, Y. Ma, S. T. Ho and G. S. Solomon, *Opt. Lett.* **27**, 948 (2002)
- [10] A. Kress, F. Hofbauer, N. Reinelt, M. Kaniber, H. J. Krenner, R. Meyer, G. Bhm and J. J. Finley, *Phys. Rev. B* **71**, 241304 (2005)
- [11] D. Englund, D. Fattal, E. Waks, G. Solomon, B. Zhang, T. Nakaoka, Y. Arakawa, Y. Yamamoto, and J. Vuckovic, *Phys. Rev. Lett.* **95**, 013904 (2005)
- [12] A. Badolato, K. Hennessy, M. Atatüre, J. Dreiser, E. Hu, P. M. Petroff and A. Imamoglu, *Science* **308**, 1158 (2005)
- [13] H. Altug, D. Englund and J. Vuckovic, *Nature Physics* **2**, 484 (2006)
- [14] W.L. Barnes, G. Björk, J.M. Gérard, P. Jonsson, J. Wasey, P. Worthing and V. Zwiller, *Eur. Phys. J. D* **18**, 197 (2002)
- [15] L. Balet, M. Francardi, A. Gerardino, N. Chauvin, B. Alloing, C. Zinoni, C. Monat, L. H. Li, N. Le Thomas, R. Houdré and A. Fiore, *Appl. Phys. Lett.* **91**, 123115 (2007)
- [16] K. Nozaki, S. Kita and T. Baba, *Optics Express* **15**, 7506 (2007)
- [17] M. Makarova, V. Sih, J. Warga, R. Li, L. Dal Negro and J. Vuckovic, *Appl. Phys. Lett.* **92**, 161107 (2008)
- [18] A. Michon, R. Hostein, G. Patriarche, N. Gogneau, G. Beaudoin, A. Beveratos, I. Robert-Philip, S. Laurent, S. Sauvage, P. Boucaud, and I. Sagnes, *J. Appl. Phys.* **104**, 043504 (2008)
- [19] Y. Akahane, T. Asano, B. S. Song, and S. Noda, *Nature (London)* **425** 944 (2003)
- [20] A. Talneau, K. H. Lee, S. Guilet and I. Sagnes, *Appl. Phys. Lett.* **92**, 061105 (2008)
- [21] K. H. Lee, S. Guilet, G. Patriarche, I. Sagnes and A. Talneau, *J. Vac. Sci. Technol. B* **26**, 1326 (2008)
- [22] R. Hostein, A. Michon, G. Beaudoin, N. Gogneau, I. Robert-Philip, I. Sagnes and A. Beveratos, *Appl. Phys. Lett.* **93**, 073106 (2008)
- [23] M. P. van Exter, G. Nienhuis, and J. P. Woerdman, *Phys. Rev. A* **54**, 3553 (1996)
- [24] Y. Xu, R. K. Lee, and A. Yariv, *Phys. Rev. A* **61**, 033807 (2000)
- [25] L. Besombes and K. Kheng L. Marsal and H. Mariette, *Phys. Rev. B* **63**, 155307 (2001)